

# Two Types of *Chlamydomonas* Flagellar Mutants Missing Different Components of Inner-Arm Dynein

Ritsu Kamiya,\* Eiji Kurimoto,\* and Etsuko Muto‡

\*Department of Molecular Biology, School of Science, Nagoya University, Nagoya 464-01, Japan; and ‡Department of Ultrastructural Research, The Tokyo Metropolitan Institute of Medical Science, Tokyo 113, Japan

**Abstract.** Two types of *Chlamydomonas reinhardtii* flagellar mutants (*idaA* and *idaB*) lacking partial components of the inner-arm dynein were isolated by screening mutations that produce paralyzed phenotypes when present in a mutant missing outer-arm dynein. Of the currently identified three inner-arm subspecies I1, I2, and I3, each containing two heterologous heavy chains (Piperno, G., Z. Ramanis, E. F. Smith, and W. S. Sale. 1990. *J. Cell Biol.* 110:379–389), *idaA* and *idaB* lacked I1 and I2, respectively. The 13 *idaA* isolates comprised three genetically different groups (*ida1*, *ida2*, *ida3*) and the two *idaB* isolates comprised a single group (*ida4*). In averaged cross-section electron micrographs, inner dynein arms in wild-type axonemes appeared to have two projections

pointing to discrete directions. In *ida1–3* and *ida4* axonemes, on the other hand, either one of them was missing or greatly diminished. Both projections were weak in the double mutant *ida1–3* × *ida4*. These observations suggest that the inner dynein arms in *Chlamydomonas* axonemes are aligned not in a single straight row, but in a staggered row or two discrete rows. Both *ida1–3* and *ida4* swam at reduced speed. Thus, the inner-arm subspecies missing in these mutants are not necessary for flagellar motility. However, the double mutants *ida1–3* × *ida4* were nonmotile, suggesting that axonemes with significant defects in inner arms cannot function. The inner-arm dynein should be important for the generation of axonemal beating.

THE inner and outer dynein arms in cilia and flagella are key protein assemblies that cause sliding between doublet microtubules (Gibbons, 1981). *Chlamydomonas* outer dynein arm contains three high molecular weight peptides (HMWs)<sup>1</sup> with ATP-hydrolyzing activities, as well as several other proteins with lower molecular weights (Piperno and Luck, 1979; King and Witman, 1989). These proteins are assembled to form a three-headed, bouquetlike structure (Johnson and Wall, 1983; Witman et al., 1983; Goodenough and Heuser, 1984), and arranged at every 24 nm along the length of the outer-doublet microtubules. The inner arm, on the other hand, is more complex. It also contains several HMWs with the ATPase activities (Huang et al. 1979; Piperno and Luck, 1979, 1981; Piperno, 1988), but comprises two morphologically different species called dyads and triads (Goodenough and Heuser, 1985). Recently, Piperno et al. (1990) have presented evidence that there actually are three species of inner-arm dynein (called I1, I2, and I3), each containing two HMWs; there are six inner-arm heavy chains altogether. From structural analyses of mutants, they have suggested that the three species are

aligned longitudinally in the order of I1-I2-I3, and the cluster of the three repeats every 96 nm.

Functional properties of the inner and outer dynein arms remain to be clarified. Specific removal of the outer dynein arm from sea urchin sperm axonemes results in a twofold reduction in reactivated motility and axonemal ATPase activity (Gibbons and Gibbons, 1973; Yano and Miki-Noumura, 1981). These observations support the view that the two types of arms perform almost identical functions in axonemal motility. However, studies with *Chlamydomonas* mutants have suggested that the two types of arms have somewhat different functions (Okagaki and Kamiya, 1986; Brokaw and Kamiya, 1987; Kamiya et al., 1989; Kagami and Kamiya, 1990). For example, mutations in inner arm lead to reduction in shear amplitude (amplitude of microtubule sliding) whereas those in outer arm result in reduction in the beat frequency (Brokaw and Kamiya, 1987).

For a definite comparison between the inner- and outer-arm functions, mutant axonemes devoid of either of the arms should be of great value. Mitchell and Rosenbaum (1985) and we (Kamiya and Okamoto, 1985; Kamiya, 1988) reported the isolation and characterization of outer arm-missing *Chlamydomonas* mutants (*pf28* and *odas*) that retained reduced motility. More recently, we isolated two types of motile mutants (*idaA* and *idaB*; previously named *ida* and *idb*, respectively) missing partial structure of the inner dynein arm

Dr. Muto's present address is Aichi Prefectural University of Fine Art, Aichi 480-11, Japan.

1. *Abbreviations used in this paper:* HMW, high molecular weight peptides; I-projection, inner projection; O-projection, outer projection; wt, wildtype.

and described their properties briefly in a review (Kamiya et al., 1989). The present report describes the isolation and characterization of these mutants in more detail. We show that wild-type inner dynein arms appear to comprise two discrete rows of subunits, either one of which is predominantly missing in *idaA* and *idaB* axonemes.

## Materials and Methods

### Strains

*Chlamydomonas reinhardtii* 137c (wild type; *wt*), a mutant missing the entire outer dynein arm (*odal*), and two types of inner-arm mutants (*idaA* [*ida1-3*] and *idaB* [*ida4*]) of both mating types were used. *ida1* and *ida4* were referred to as *ida* (or *ida98*) and *idb*, respectively, in previous papers (Brokaw and Kamiya, 1987; Kamiya et al., 1989). Isolation and characterization of *odal* have been described (Kamiya and Okamoto, 1985; Kamiya, 1988).

The inner-arm mutants *ida1-3* and *ida4* were isolated from nonmotile double mutants with *odal* background in the following way. *N*-methyl-*N*-nitro-*N*-nitrosoguanidine was added to *odal* cells, which had been grown in Tris-acetic acid-phosphate (TAP) medium (Gorman and Levine, 1965) to a late logarithmic phase under constant illumination, to give a final concentration of 20  $\mu$ g/ml. After 15–45 min of the addition, the cell suspension was freed of *N*-methyl-*N*-nitro-*N*-nitrosoguanidine by centrifugation and resuspension of the cells in fresh TAP medium. 1 ml aliquots were taken from this suspension and transferred to eight test tubes ( $\sim$ 1-cm diam), each containing 3 ml of TAP medium. Cells were grown in these test tubes over a 12-h/12-h, light/dark cycle until the cells' green color thickened at the upper part of the test tubes. Cells grown at the bottom of each test tube were then carefully transferred with a Pasteur pipette to another tube containing 4 ml of fresh TAP medium. This process was repeated three times over a period of 1–2 wk. The cells grown at the bottom of the last sets of test tubes were saved, diluted, and inoculated on 1.5% TAP agar plates. The agar plates were kept under constant illumination for 3–5 d. Colonies with heaped appearances were transferred with toothpicks to 96-well cell culture plates, each well containing 0.2 ml of liquid TAP medium. Usually 48 colonies were isolated from a single test tube. The plates were then placed under constant illumination for 1–2 d, after which time each well was observed with an inverted microscope. Completely nonmotile cells were saved and inoculated on TAP agar plates. 1 wk after the transfer to the agar plates, the cells were transferred to a gamete-inducing medium (Levine and Ebersold, 1960) and mated with wild-type gametes of the opposite mating type. Tetrads were obtained and analyzed according to standard procedures (Levine and Ebersold, 1960). The desired mutants were isolated from nonparental ditype tetrads, i.e., tetrads consisting of two daughter cells with *oda* phenotypes and two with an identical, slow-swimming phenotype. The latter two were saved and analyzed for the composition of flagellar axoneme. Mutants judged to be deficient in inner dynein arm were further mated with wild type, and daughter cells with both mating types were obtained. When two or more isolates from an initial test tube culture gave rise to daughter cells of similar flagellar composition, only one isolate was saved to assure that all the isolates were independent.

Double mutants were produced by a standard method of genetic crossing; desired mutants were obtained from nonparental-ditype tetrads containing two wild-type daughter cells.

### Genetic Analysis

Newly isolated mutants were examined for allelism with other inner-arm mutants by using a standard method of tetrad analysis (Levine and Ebersold, 1960). Complementation in temporary dikaryons (Starling and Randall, 1971) was not useful to determine whether a pair of mutants were allelic, because dikaryons between inner-arm mutants did not show good motility recovery even if the two mutants were nonallelic. A pair of mutants were judged to be allelic when cultures of >50 zygotes did not produce a wild-type daughter cell.

Independent inner-arm mutations were examined for genetic loci by standard procedures (Harris, 1989). Mutants on various linkage groups were obtained from Dr. Elizabeth Harris (*Chlamydomonas* Genetics Center, Department of Botany, Duke University, Durham, NC).

### Culture

Cells of *wt*, *odal*, and *ida1-4* were grown in 600 ml of TAP medium with aeration over a 12-h/12-h, light/dark cycle. Because double mutants *ida1-3*  $\times$  *odal* and *ida1-3*  $\times$  *ida4* tended to grow only short flagella when cultured in the liquid medium, they were first grown on a 300-cm<sup>2</sup>, 1.5% agar/TAP medium for  $\sim$ 1 wk, and, when growth appeared complete, transferred to 200 ml of liquid medium (Sager and Granick, 1953). The cells grew flagella after being kept aerated for 1–4 h, although the flagella were still shorter than normal (see Results).

### Isolation of Axonemes

Flagella of wild type and mutants were isolated by the method of Witman et al. (1978), using dibucaine-HCl to detach flagella from the cell bodies. The isolated flagella were demembrated by suspending in a solution containing 10 mM Hepes, 5 mM MgSO<sub>4</sub>, 1 mM DTT, 1 mM EGTA, and 0.4% NP-40 (pH 7.4).

### EM

Thin-section EM was carried out with axoneme samples fixed with 2% glutaraldehyde in the presence of 1% tannic acid. Specimens were postfixed with 1% OsO<sub>4</sub>, dehydrated through a series of ethanol solutions, and embedded in Epon 812. Golden thin sections ( $\sim$ 100-nm thick) were used. Sections were double stained with uranylacetate and lead citrate, and observed with a microscope (model JEM100C; Jeol Co., Tokyo, Japan).

To examine the shape of inner dynein arms in mutants, images of outer-doublet microtubules in cross-section micrographs were averaged using an IBAS image analyzer (Zeiss, Oberkochen, FRG). Individual images of eight outer doublets (all but the one missing the outer dynein arm; Hoops and Witman, 1983) in an enlarged cross-section micrograph of axoneme were taken with a TV camera and put into 8-frame memories of IBAS, which was equipped with 12 memories. In doing so, the orientation of the micrograph was adjusted so that each "8"-shaped doublet microtubule image matched as closely as possible an overlay reference image that had been generated by binary contrast enhancement of an arbitrarily chosen doublet image. All the images in the memory were averaged after they were judged by visual inspection to be oriented well with respect to each other. Although this method involved such a subjective process that the image orientation was checked by eye, the averaged image did not change noticeably when the whole process was performed by different operators. The averaged images, however, do not permit a quantitative analysis of the shape, because of such a subjective process involved; a quantitative analysis of the image would become possible if the image averaging is performed using a computer algorithm to take correlations between different doublet images.

### Electrophoresis

Compositions of dynein heavy chains were analyzed by SDS-PAGE using the method of Laemmli (1970), as modified by Jarvik and Rosenbaum (1980; see also Pfister et al., 1982). A 3–5% polyacrylamide gradient and a 3–8 M urea gradient were used. Gels were stained with silver (Merril et al., 1981).

### Motility and Flagellar Length

Swimming velocities of mutants were measured from video recordings of dark-field images of swimming cells, by superimposing the image on a monitor screen of a personal computer. A homemade program was used to track the position of a cell with a 'mouse.'

Flagellar beat frequencies of live cells were measured by analyzing the vibration frequency of cell bodies by means of a dark-field microscope, a photomultiplier, and an FFT analyzer, as described elsewhere (Kamiya and Hasegawa, 1987). All the measurements were carried out at 25°C.

For measurement of flagellar lengths, flagella were detached from the cell body by treatment with 5 mM dibucaine-HCl, and their images were taken with a TV camera. Average flagellar length was obtained by measuring the lengths of >50 flagellar images on the monitor. This procedure yielded the flagellar average length in flagellated cells, not in the whole cell population; in double mutants such as *ida1*  $\times$  *odal*, only 10–30% of cells were usually flagellated and thus the average length in the total population of cells should be much shorter.

## Results

### Isolation of Inner-Arm Mutants

Soon after we started isolating dynein-arm mutants by screening cells that tended to grow at the bottom of a test tube culture, we came to notice that mutants deficient in inner dynein arms were more rarely obtained than outer-arm mutants; of ~100 slow swimmers obtained, only two were found to be inner arm-deficient mutants, whereas 35 were outer arm-missing mutants of 10 different complementation groups (*odas*; Kamiya, 1988). We therefore used another method to isolate inner-arm mutants. This method, based on our presumption that a mutant with defects in both outer arm and inner arm would be nonmotile, comprised two steps: isolation of nonmotile double-mutants from mutagenized *oda1* cells, and removal of the *oda1* background by back-cross of the double mutants with wild type. This procedure proved to be effective for isolation of certain types of inner-arm mutants; of ~70 nonmotile double-mutants that underwent mating with wild type, at least 25 appeared to have defects in the inner arm in addition to the *oda1* mutation. SDS-PAGE analyses (see below) of axonemes indicated that the second mutations in 15 of the 25 double mutants had stable phenotypes and can be classified into two types which we call *idaA* (13 strains) and *idaB* (2 strains). Some of the other inner-arm mutations found in these isolates had defects distinct from those in *idaA* or *idaB*. For example, one type of mutant was missing No. 4 heavy chain which are present in both *idaA* and *idaB* axonemes (for the nomenclature of heavy chains; Fig. 1). These mutants may have defects in a third inner-arm subspecies, although we were unable to assign the No. 4 HMW band to one of the three inner arm subspecies that have been identified with an SDS-PAGE system different from ours (Piperno et al., 1990). We did not use them in this study because of their somewhat variable phenotypes.

### Genetic Analyses

Genetic crosses between these strains indicated that these *idaA* strains comprised three groups *ida1*-3, while the two *idaB* strains comprised one group *ida4* (Table I). As reported before, *ida1* is allelic to *pf30*, a similar mutant isolated by Huang, Ramanis, and Luck (Brokaw and Kamiya, 1987). Al-

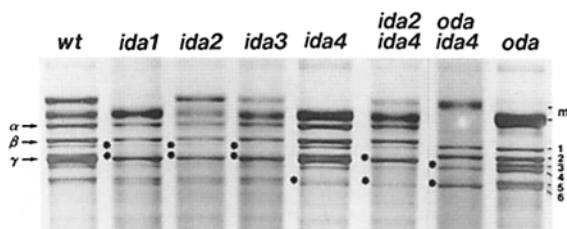


**Figure 1.** Portions of 3–5% SDS-urea-PAGE patterns showing the high molecular weight bands of mutant and wild-type axonemes. *wt*, wild type; *ida2/ida4*, recombinant between *ida2* and *ida4*; *oda/ida4*, recombinant between *oda1* and *ida4*; *oda*, *oda1*. (\*) indicate inner-arm bands missing or diminished in mutant axonemes.  $\alpha$ ,  $\beta$ , and  $\gamma$  indicate outer-arm heavy chains. (*m*) Bands with contaminating membrane proteins. Stained with silver.

**Table I. Classification of Inner-Arm Mutants**

Type	Genetic group	Linkage group	Strains (isolation numbers)
<i>idaA</i>	<i>ida1</i>	XII	98,* 114, 116, 138, 146, 177, ( <i>pf30</i> )*
	<i>ida2</i>	XV	124,* 131, 132, 133, 135
	<i>ida3</i>	III	129, 206*
<i>idaB</i>	<i>ida4</i>	XII	166,* 168

\* Used as the exemplar strain for each group.

† Isolated by Huang, Ramanis, and Luck (Piperno, 1988).

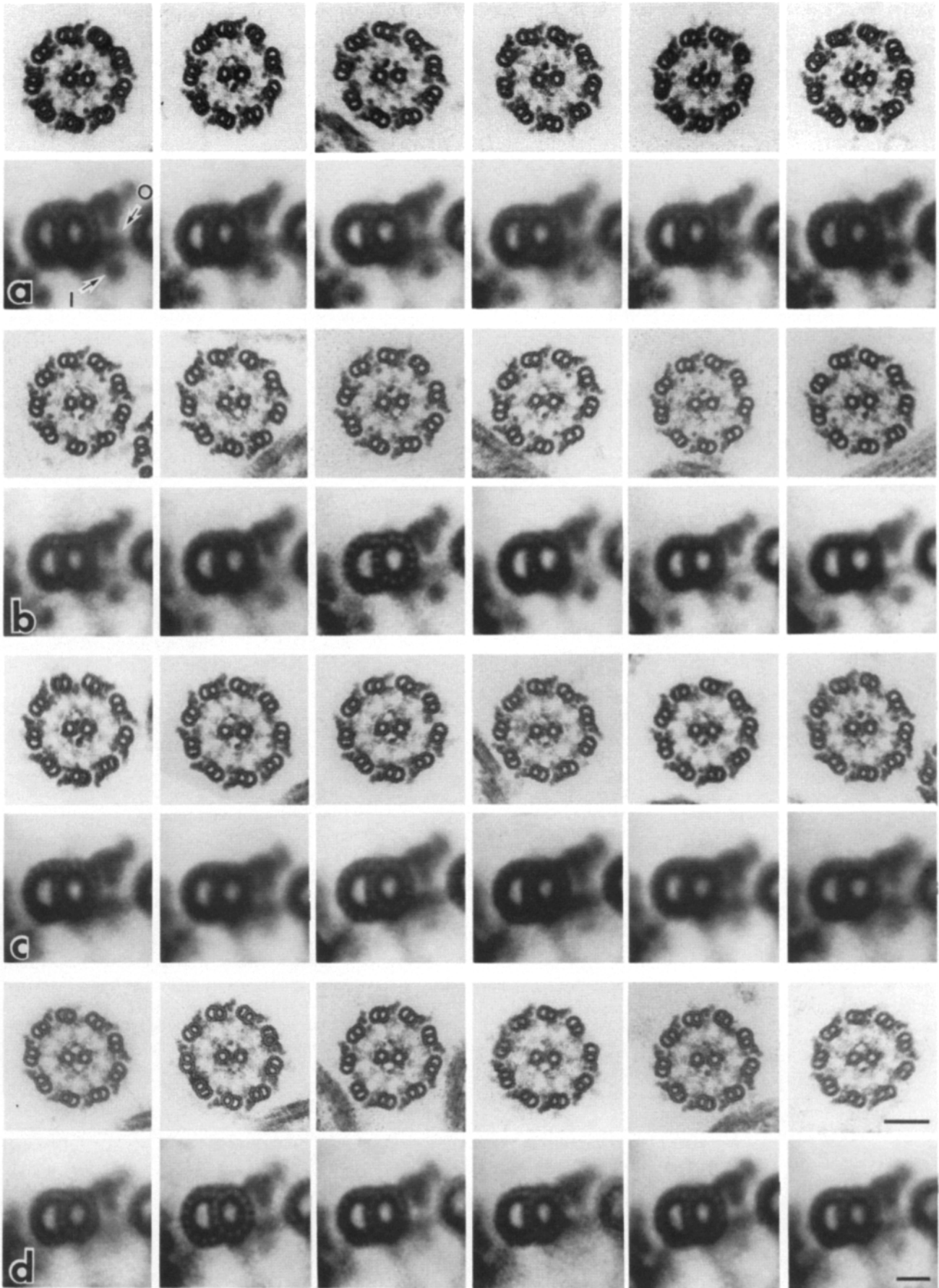
though *pf30* had been mapped to linkage group IX (see Harris, 1989), we found *ida1* and *pf30* were linked with *lf2* on linkage group XII (*ida1*  $\times$  *lf2*: parental ditype: nonparental ditype: tetratype = 130:0:8). Also, *ida2* was linked with *nicl* on linkage group XV (58:0:3), and *ida3* with *acl7* (18:0:2) and *pf15* (8:0:15) on linkage group III. Another type of inner-arm mutant *ida4* was found to be closely linked with *ida1* (201:0:2) and *lf2* (162:0:5). Therefore, *ida1*, *ida4*, and *lf2* must be all located within a region of 2–3 cM at the left end of linkage group XII.

### Axoneme Compositions

The SDS-PAGE pattern in Fig. 1 shows the difference in HMWs between wild-type and mutant axonemes. As reported previously (Piperno and Luck, 1979; Pfister et al., 1982), HMW bands of both inner- and outer-arm dyneins occurred in a small region corresponding to the molecular mass of 400–450 kD. (One or two strong bands often appeared just above these dynein bands, marked by *m* in Fig. 1. These are those with contaminating membrane proteins which tended to be strongly stained with silver.) The wild-type pattern contained three outer-arm bands ( $\alpha$ ,  $\beta$ , and  $\gamma$ ), which were more intense than the inner-arm dynein bands. These bands were entirely absent from the *oda* pattern.

In *ida1*-3 axonemes, two bands (No. 1 and No. 2) between  $\beta$  and  $\gamma$  outer-arm bands are either missing or greatly diminished. The amount of residual No. 1 chain was slightly variable among different preparations of axonemes and among different strains, although it was constantly small compared with that of wild type. No. 2 band was missing from all of the *ida1*-3 axonemes. However, it was frequently difficult to identify this band in wild type and *oda1* axonemes because of the overlap with the outer-arm  $\gamma$  chain and No. 3 inner-arm chain. On the other hand, *ida4* axonemes had a reduced No. 5 band. In addition, this mutant appeared to lack another band (No. 3) that was overlapped with the outer-arm  $\gamma$  chain; in the double mutant *ida4* and *oda1*, this band was clearly missing. Three bands (No. 1, No. 2, and No. 5) were absent or weakened in the double mutant *ida2*  $\times$  *ida4*, although No. 1 band was not as totally absent as in the single mutant. The pattern of this double mutant was similar to that of the axoneme of a previously isolated mutant, *pf23*, except that the latter also lacked No. 4 band (Huang et al., 1979; Kamiya, R., unpublished observation). No. 3 band may also be missing in the double mutant; however, this was not confirmed because the triple mutant *ida2*  $\times$  *ida4*  $\times$  *oda1* did not yield enough flagella for the analysis.

Besides the defects in the heavy chains, the inner arm



mutants may well be missing some light chains and intermediate-sized chains. Although this possibility has not been made clear in the present study using one dimensional SDS-PAGE of axonemes, a study with fractionated dynein samples from mutants in fact indicates that *ida1* lacks a peptide of 140 kD and *ida4* lacks a peptide of ~30 kD (Kagami, O., and R. Kamiya, unpublished observations). More detailed analysis of the defects in lower molecular weight chains associated with the inner-arm mutations is now in progress.

### Electron Microscope Images of Mutant Axonemes

Thin-section EM showed that both *ida1-3* and *ida4* axonemes retained inner-arm images, but that the inner-arm images in the mutants were weaker than in wild type (Kamiya et al., 1989). To look more closely at the inner-arm image, we averaged the cross-section images of doublet microtubules in mutant and wild-type axonemes using an image processor. Image averaging could be carried out by printing a cross-section image nine times, each time rotating the image by 360/9° around the center of the axoneme (Markham et al., 1963). However, this procedure often results in a blurred image, because the outer doublets in cross-section micrographs are rarely positioned on an exact circle. We therefore averaged images of eight doublet microtubules (all the outer doublets but one that does not bear the outer dynein arm; Hoops and Witman, 1983) by superimposing the cross-section image of an outer doublet on that of another using a TV camera and an image processor (see Materials and Methods for details; see also Afzelius et al., 1990 for an improved technique).

Fig. 2 shows a gallery of cross-section micrographs of *wt*, *ida1-3*, *ida4*, and *ida2 × ida4* axonemes together with the averaged doublet images. To show the extent of image variation, we present six sets of the original and processed images for each kind of axoneme. The micrographs used had been chosen only on the basis of whether all the nine outer doublets appeared clearly; no selection had been made on the basis of the appearance of the inner arm in the original and processed micrographs.

Such averaging clearly revealed differences between wild-type and mutant axonemes in their inner-arm images. In *wt* (Fig. 2 a), the inner arms appear to have two discrete projections, one pointing directly toward the adjacent doublet microtubule—outer (O)—projection—and the other to the inner part of the axoneme—inner (I)—projection. These two projections must not be artificial images resulted from the averaging, since they were frequently identifiable on individual outer-doublets in the original micrograph.

In *ida1-3* (Fig. 3 b), the O-projection is missing or replaced by a thin fibrous structure, much weaker in intensity than the O-projection observed in *wt* axoneme. Because the thin fibre spans the entire distance between two adjacent outer doublets, we suppose its major part is the inter-doublet link, which can be observed in *wt* axonemes after extraction of dynein arms (Warner, 1983; Goodenough and Heuser,

Table II. Motility and Flagellar Length in Dynein-arm Mutants

	Flagellar length	Swimming velocity	Beat frequency
	$\mu\text{m}$	$\mu\text{m/s}$	Hz
<i>wt</i>	11.1 ± 1.9	155.0 ± 23.3	63
<i>oda1</i>	11.4 ± 2.0	58.0 ± 7.5	29
<i>ida1</i>	10.9 ± 1.6	82.1 ± 13.8	50
<i>ida2</i>	11.0 ± 1.2	77.7 ± 15.2	54
<i>ida3</i>	10.2 ± 1.8	77.3 ± 11.0	45
<i>ida4</i>	9.4 ± 1.6	102.2 ± 10.7	62
<i>ida2 × ida4</i>	7.9 ± 3.4		Nonmotile
<i>ida1 × oda1</i>	3.0 ± 0.8		Nonmotile
<i>ida4 × oda1</i>	5.6 ± 2.4		Nonmotile

Flagellar lengths and swimming velocities are those averaged from more than 50 measurements and expressed as mean ± SD. Beat frequency was measured by analyzing the bodily vibration of cells with a fast Fourier transform analyzer (Kamiya and Hasegawa, 1987); the median value of the frequency peak is shown for each strain. Motility was measured at 25°C.

1989). In contrast to *ida1-3*, *ida4* axoneme lacks the I-projection (Fig. 2 c). The degree of the deficiency is slightly variable from an image of axoneme to another and some of the images show a low electron density in the I-projection region. However, the prominent globular appendage of the I-projection observed in *wt* and *ida1-3* is consistently missing in all the micrographs of *ida4* axoneme. In the double mutant *ida2 × ida4* (Fig. 2 d), both of the two projections are weaker than the *wt* axoneme, although the image is somewhat variable. This kind of axoneme often has the O-projection as in the *ida4* axoneme. The occurrence of the O-projection may be because of the presence of the No. 1 band (see above) in this double mutant.

### Motility Characteristics

All the mutants we isolated were motile (Table II). Therefore, neither the parts of inner arms missing in these mutants nor the entire outer arm (Kamiya and Okamoto, 1985; Mitchell and Rosenbaum, 1985) is necessary for flagellar motility. As Table II shows, *ida4* had the same beat frequency as the wild type but its swimming velocity was ~2/3 of the normal value. This suggests that the *ida4* mutation affected the flagellar waveform. Brokaw and Kamiya (1987) reported that *ida1* flagella had a shear amplitude reduced to ~70% of the normal value. It is likely that *ida4* also had a reduced shear amplitude, although this conclusion must await waveform analysis.

Since *ida1-3* and *ida4* were isolated by screening nonmotile double mutants with *oda1*, the double mutants *ida1-3 × oda1* and *ida4 × oda1* were naturally nonmotile; these double mutants had short flagella that were almost completely motionless. Unexpectedly, however, the double mutants between the two types of motile inner-arm mutants (*ida1-3 × ida4*) were also found to have lost motility; their flagella showed only erratic twitching movements. This observation

Figure 2. Gallery of cross-section axoneme images and averaged images of the outer doublets in these photographs. (a) wild type; (b) every two photographs from left to right *ida1*, *ida2*, and *ida3*; (c) *ida4*; and (d) double mutant *ida2 × ida4*. Arrows in the upper left photograph indicate the I- and O-projections of the inner arm image. Note that the O-projection is greatly weakened in b, whereas the I-projection is weakened in c. Bars: (top) 0.1  $\mu\text{m}$ ; (bottom) 0.02  $\mu\text{m}$ .

suggests that axonemes with large defects in the inner arm are incapable of beating.

## Discussion

### Mutants Missing Inner-arm Components

In the present study we developed a new procedure for isolation of inner dynein arm mutations and thereby obtained two types of mutants (*idaA* and *idaB*) missing different subsets of HMWs. The 13 *idaA*-type strains isolated were found to comprise three genetically different groups, which were named *ida1*, *ida2*, and *ida3*. *ida1* was found to be the allele of *pf30*, a mutant isolated by Huang, Ramanis and Luck and used in previous studies on inner-arm structure and function (Piperno, 1988; Brokaw and Kamiya, 1987; Goodenough et al., 1987). The other two *idaA*-type mutants *ida2* and *ida3* are reported here for the first time. The two isolates of *idaB* comprised a genetically single group *ida4*, which has been described only briefly in a previous study (Kamiya et al., 1989).

Piperno et al. (1990) have reported that the inner arm is composed of three species I1, I2, and I3, each containing two HMWs, and that *pf30* (*ida1*) lacks I1 and *pf23* both I1 and I2. Since the SDS-PAGE pattern of *ida1-3* × *ida4* axoneme is similar to that of *pf23*, it is likely that *ida4* lacks the two I2 heavy chains. Piperno, G. (personal communication) has found this is actually the case; using an improved SDS-PAGE system, he has found that *ida4* is missing one (chain 2'; Piperno, G., et al., 1990) of the two I2 heavy chains and has a reduced amount of the other (chain 2).

### Inner-Arm Structure

The averaged cross-section images of *wt* and mutant axonemes (Fig. 2 *a*) clearly demonstrated the presence of two distinct projections in the inner arms, one (O-projection) pointing directly toward the adjacent outer-doublet and the other (I-projection) toward the inner space of the axoneme. The former projection is greatly weakened in *ida1-3* (Fig. 2 *b*) that lack the I1 subspecies and the latter in *ida4* that lacks the I2 subspecies (Fig. 2 *c*). These observations indicate that the three inner-arm subspecies are aligned not in a straight line within an axoneme, but rather in a staggered row, or in two discrete rows with the I1 subspecies in the outer row and the I2 subspecies in the inner row. In fact, a recent study using extensive series of thin-section tilt-series electron micrographs is suggesting that the inner dynein arms in *Chlamydomonas* do occur in two parallel rows (Muto et al., 1989; and manuscript in preparation).

Piperno et al. (1990) have indicated that the three inner-arm subspecies, I1, I2, and I3, are longitudinally aligned in the order of I1-I2-I3 repeating every 96 nm; they have shown that a gap is present at every 96 nm in the inner-arm row of wild type, and that this gap is wider in *pf30* (*ida1*) lacking I1 and still wider in another mutant *pf23* lacking both I1 and I2. Although our present finding does not directly argue against their general conclusion, it suggests that a model with the three inner-arm species in line is too simple. Moreover, an alternative view that the three species are aligned in a staggered row seems to have some difficulty in explaining observed image intensities of the arms. In the micrographs of thin sections about 100-nm thick, which

should contain all the dynein arm components within a repeat distance of 96 nm, the two inner-arm projections in *wt* are similar in electron density to each other and to the outer arm (Fig. 2 *a*). On the other hand, if there are only three inner-arm subspecies aligned in a staggered row within the repeat distance, one of the two inner-arm projections seen in an axoneme cross section may well contain only one subspecies (containing two heavy chains) within the repeat unit, in which as many as four outer arms (each containing three heavy chains) are present. Thus, it would be difficult to explain the similar image intensity between the inner and outer arms by a simple staggered row model, unless we assume that some inner arm subspecies has a shape elongated in the direction of the axoneme length, or that the staining of the dynein arms is not linearly related with their actual mass.

The exact arrangement of the inner arm subspecies, however, must await further studies. One problem with our present study is that it gives us no clues about the localization of the third subspecies I3. The cross section micrographs of *ida2* × *ida4* axoneme (Fig. 2 *d*) show weakened inner-arm images which may represent the location of I3. However, this double mutant retains No. 1 HMW (a component of I1) (Fig. 1), and its inner-arm appearance is variable from a very faint one to the one similar to the image of *ida4* inner arm (Fig. 2 *d*). Thus the O-projection observed in this double-mutant might well be because of the presence of the No. 1 chain as well as of I3. Mutants missing both I1 and I2 completely, or those missing I3, will be necessary to locate I3.

We have tried to establish the inner-arm organization by observing the inner-arm images of mutants in longitudinal sections in the course of this study. However, the images we obtained varied so greatly from one axoneme to another that we were unable to reach a unified view. We think this difficulty is expected if the inner arm comprises two rows; if so, an inner-arm image in any longitudinal section should be that of the two rows superimposed, and this should vary greatly depending on the viewing angle. Hence, further studies using tilt series electron micrographs of various dynein mutants will be necessary to determine the organization of different inner-arm subspecies.

### Motility in Inner-Arm Mutants

Both *ida1-3* and *ida4*, as well as the outer arm-missing mutant *odal*, were able to swim although more slowly than *wt*. Thus neither the part of the inner dynein arm missing in *ida1-3* and *ida4* nor the entire outer arm is necessary for generation of flagellar beating. However, the double mutant *ida1-3* × *ida4* was paralyzed, as were double mutants *ida1-3* × *odal* and *ida4* × *odal*. These results indicate that the inner-arm subsets and the outer dynein arm are functionally interdependent and axonemes lacking a large part of the inner arm cannot beat. This idea agrees with the observation that a mutant (*pf23*) missing the I1 and I2 inner-arm subspecies is paralyzed (Huang et al., 1979).

Recently we have found that the *ida2* × *ida4* axoneme can undergo sliding disintegration when perfused with protease and ATP, at a velocity as high as that in *wt* (Kurimoto and Kamiya, manuscript in preparation). Hence the lack of motility in the *ida2* × *ida4* axoneme may be because of a defect in the mechanism that organizes microtubule sliding into regular axonemal beating, rather than a defect in the force

production itself. It would be interesting to examine whether *ida1-3* × *oda1* and *ida4* × *oda1* axonemes also can undergo sliding disintegration, and furthermore, to inquire by physiological experiments whether the defect in those mutants is in the initiation of bend formation or in the propagation of bend that is formed at the base.

Our studies on dynein-arm mutants have so far shown that no single species of axonemal dynein is essential to the generation of motility. Whether the third inner arm subpecies I3 is essential has remained an important question.

We thank Drs. Hirokazu Hotani, Tomohiko Ito, Haruto Nakayama, and Nobuhiro Kamiike of Laboratory of Exploratory Research for Advanced Technology (Kyoto) for allowing us to use their IBAS image processor. Dr. Gianni Piperno (Rockefeller University, New York) kindly sent us a manuscript before publication. We are also grateful to him and Dr. Winfield Sale (Emory University School of Medicine, Atlanta, GA) for critically reading an early version of the manuscript, and to Dr. Elizabeth Harris (Duke University, Durham, NC) for sending us various mutants used for genetic analyses.

This study has been supported by grants-in-aid from the Ministry of Education, Science and Culture of Japan (01657001, 02239101) to R. Kamiya.

Received for publication 27 June 1990 and in revised form 16 October 1990.

## References

- Afzelius, B., P. L. Bellon, and S. Lanzavecchia. 1990. Microtubules and their protofilaments in the flagellum of an insect spermatozoon. *J. Cell Sci.* 95:207-217.
- Brokaw, C. J., and R. Kamiya. 1987. Bending patterns of *Chlamydomonas* flagella. IV. Mutants with defects in inner and outer dynein arms indicate differences in dynein arm function. *Cell Motil. and Cytoskeleton.* 8:68-75.
- Gibbons, I. R. 1981. Cilia and flagella of eukaryotes. *J. Cell Biol.* 91:107s-124s.
- Gibbons, B. H., and I. R. Gibbons. 1973. The effects of partial extraction of dynein arms on the movement of reactivated sea-urchin sperm. *J. Cell Sci.* 13:337-357.
- Goodenough, U. W., and J. E. Heuser. 1984. Structural comparison of purified dynein proteins with in situ dynein arms. *J. Mol. Biol.* 180:1083-1118.
- Goodenough, U. W., and J. E. Heuser. 1985. Substructure of inner dynein arm, radial spokes, and the central pair/projection complex of cilia and flagella. *J. Cell Biol.* 100:2008-2018.
- Goodenough, U. W., and J. E. Heuser. 1989. Structure of soluble and in situ ciliary dyneins visualized by quick-freeze deep-etch microscopy. *In Cell Movement.* Vol. 1. F. D. Warner, P. Satir, and I. R. Gibbons, editors. Alan R. Liss, Inc. New York. 121-140.
- Goodenough, U. W., B. Gebhart, V. Mermal, D. Mitchell, and J. Heuser. 1987. High-pressure liquid chromatography fractionation of *Chlamydomonas* dynein extracts and characterization of inner-arm dynein subunits. *J. Mol. Biol.* 194:481-494.
- Gorman, D. S., and R. P. Levine. 1965. Cytochrome F and plastocyanin: their sequence in the photosynthetic electron transport chain of *Chlamydomonas reinhardtii*. *Proc. Natl. Acad. Sci. USA.* 54:1665-1669.
- Harris, E. 1989. The *Chlamydomonas* Sourcebook. Academic Press Inc., Orlando, FL. 780 pp.
- Hoops, H. J., and G. B. Witman. 1983. Outer doublet heterogeneity reveals structural polarity related to beat direction in *Chlamydomonas* flagella. *J. Cell Biol.* 97:902-908.
- Huang, B., G. Piperno, and D. J. L. Luck. 1979. Paralyzed flagella mutants of *Chlamydomonas reinhardtii* defective for axonemal doublet microtubule arms. *J. Biol. Chem.* 254:3091-3099.
- Jarvik, J. W., and J. L. Rosenbaum. 1980. Oversized flagellar membrane protein in paralyzed mutants of *Chlamydomonas reinhardtii*. *J. Cell Biol.* 85:258-272.
- Johnson, K. A. 1985. Pathway of the microtubule-dynein ATPase and the structure of dynein: a comparison with myosin. *Annu. Rev. Biophys. Biophys. Chem.* 14:161-188.
- Johnson, K. A., and J. S. Wall. 1983. Structure and molecular weight of the dynein ATPase. *J. Cell Biol.* 96:669-678.
- Kagami, O., and R. Kamiya. 1990. Strikingly low ATPase activities in flagellar axonemes of a *Chlamydomonas* mutant missing outer dynein arms. *Eur. J. Biochem.* 187:441-446.
- Kamiya, R. 1988. Mutations at twelve independent loci result in absence of outer dynein arms in *Chlamydomonas reinhardtii*. *J. Cell Biol.* 107:2253-2258.
- Kamiya, R., and E. Hasegawa. 1987. Intrinsic difference in beat frequency between the two flagella of *Chlamydomonas reinhardtii*. *Exp. Cell Res.* 173:299-304.
- Kamiya, R., and M. Okamoto. 1985. A mutant of *Chlamydomonas reinhardtii* that lacks the flagellar outer dynein arm but can swim. *J. Cell Sci.* 74:181-191.
- Kamiya, R., E. Kurimoto, H. Sakakibara, and T. Okagaki. 1989. A genetic approach to the function of inner and outer arm dynein. *In Cell Movement* Vol. 1. F. D. Warner, P. Satir, and I. R. Gibbons, editors. Alan R. Liss, Inc., New York. 209-218.
- King, S. M., and G. B. Witman. 1989. Molecular structure of *Chlamydomonas* outer arm dynein. *In Cell Movement* Vol. 1. F. D. Warner, P. Satir, and I. R. Gibbons, editors. Alan R. Liss, Inc., New York. 61-75.
- Laemmli, U. K. 1970. Cleavage of structural proteins during the assembly of the head of bacteriophage T4. *Nature (Lond.)* 227:680-685.
- Levine, R. P., and W. T. Ebersold. 1960. The genetics and cytology of *Chlamydomonas*. *Ann. Rev. Microbiol.* 14:197-216.
- Luck, R. A., and G. Piperno. 1989. Dynein arm mutants of *Chlamydomonas reinhardtii*. *In Cell Movement* Vol. 1. F. D. Warner, P. Satir, and I. R. Gibbons, editors. Alan R. Liss, Inc., New York. 49-60.
- Markham, R., S. Frey, and G. J. Hills. 1963. Methods for the enhancement of image details and accentuation of structure in electron microscopy. *Virology.* 20:88-102.
- Merrill, C. R., D. Goldman, S. A. Sedman, and M. H. Ebert. 1981. Ultrasensitive stain for proteins in polyacrylamide gels shows regional variation in cerebrospinal fluid protein. *Science (Wash. DC)* 211:1437-1438.
- Mitchell, D. R., and J. L. Rosenbaum. 1985. A motile *Chlamydomonas* flagellar mutant that lacks outer dynein arms. *J. Cell Biol.* 100:1228-1234.
- Muto, E., R. Kamiya, and S. Tsukita. 1989. Structure of inner dynein arms in *Chlamydomonas* flagella. *J. Muscle Res. Cell Motil.* 10:269.
- Okagaki, T., and R. Kamiya. 1986. Microtubule sliding in mutant *Chlamydomonas* devoid of outer or inner dynein arms. *J. Cell Biol.* 103:1895-1902.
- Pfister, K. K., R. B. Fay, and G. B. Witman. 1982. Purification and polypeptide composition of dynein ATPase from *Chlamydomonas* flagella. *Cell Motil. and Cytoskeleton.* 2:525-547.
- Piperno, G. 1988. Isolation of a sixth dynein subunit adenosine triphosphatase of *Chlamydomonas* axonemes. *J. Cell Biol.* 106:133-140.
- Piperno, G., and D. J. L. Luck. 1979. Axonemal adenosine triphosphatases from flagella of *Chlamydomonas reinhardtii*: purification of two dyneins. *J. Biol. Chem.* 254:3084-3090.
- Piperno, G., and D. J. L. Luck. 1981. Inner arm dynein from flagella of *Chlamydomonas reinhardtii*. *Cell.* 27:331-340.
- Piperno, G., Z. Ramanis, E. F. Smith, and W. S. Sale. 1990. Three distinct inner dynein arms in *Chlamydomonas* flagella: molecular composition and location in the axoneme. *J. Cell Biol.* 110:379-389.
- Sager, R., and S. Granick. 1953. Nutritional studies with *Chlamydomonas reinhardtii*. *Ann. NY Acad. Sci.* 56:831-838.
- Starling, D., and J. Randall. 1971. The flagella of temporary dikaryons of *Chlamydomonas reinhardtii*. *Genet. Res.* 18:107-113.
- Warner, F. D. 1983. Organization of interdoublet links in Tetrahymena cilia. *Cell Motil. and Cytoskeleton.* 3:321-332.
- Witman, G. B., J. Plummer, and G. Sander. 1978. *Chlamydomonas* flagellar mutants lacking radial spokes and central tubules. Structure and function of specific axonemal components. *J. Cell Biol.* 76:729-747.
- Witman, G. B., K. A. Johnson, K. K. Pfister, and J. S. Wall. 1983. Fine structure and molecular weight of the outer dyneins of *Chlamydomonas*. *J. Submicrosc. Cytol.* 15:193-198.
- Yano, Y., and T. Miki-Noumura. 1981. Recovery of sliding ability in arm-depleted flagellar axonemes after recombination with extracted dynein 1. *J. Cell Sci.* 48:223-239.